Final-State Interactions in Quasifree Electron Scattering from Nuclei*

C. D. Epp and T. A. Griffy
Department of Physics, The University of Texas, Austin, Texas 78712
(Received 22 December 1969)

The effect of strong final-state interactions on the process $A(e,e'p)B$ is investigated. Cross sections for this process are calculated for various bound-state proton wave functions, and an optical-model potential is used to describe the final-state interaction.

INTRODUCTION

The quasifree process $A(p, 2p)B$ has been widely used in nuclear structure studies,[1] particularly for investigations of the outer shells of nuclei. However, protons are strongly interacting particles, and thus it is difficult to separate the scattering mechanism from nuclear structure effects. Electrons are preferable to protons as projectiles because they interact electromagnetically and not strongly, and the electromagnetic interactions are well understood. Although quasifree electron scattering experiments are difficult to perform because of the smallness of the electromagnetic cross sections, quasifree electron scattering from Be, C, Al, S, Ca, and As has been performed at Frascati,[2-6] and quasifree electron-proton scattering in H^2, H^3, and He^3 has been performed at Stanford[7,8] and Orsay.[9] More and better experimental results are needed for quasifree electron scattering. These experiments should be easier to perform in the near future, as electron accelerators with high current and high duty cycle begin operation.

Since quasifree electron scattering is an electromagnetic, high-energy process, a good first approximation to the cross section can be calculated using the Born approximation (BA) corresponding to the diagram of Fig. 1. A necessary correction to the Born approximation is the effect of final-state interactions between the emerging proton and the residual nucleus. Preliminary investigations of final-state interactions were performed by Jacob and Maris[10] who used a WKB approximation to show that the essential effect of the final-state interactions was just to reduce the size of the cross section. Most of the theoretical calculations which have been done for quasifree electron scattering, have used the Born approximation or, following Jacob and Maris, some reduction factor times the Born approximation. Wyatt has shown that the effects of final-state interactions can be simulated by using an effective momentum in the expression for the cross section calculated in the impulse approximation.[11]

In the calculations presented below, the final-state interactions between the outgoing proton and the residual nucleus are described by an optical-model potential.[12] The wave function for the final proton is expanded in partial waves, and the radial part of the function is obtained from a numerical integration of the radial Schrödinger equation. The optical parameters used in the calculation were obtained from experimental results of elastic proton scattering from whatever residual nucleus one is considering. If data on the desired nucleus were not available, results for a similar nucleus were used. Because of their analytic simplicity, all previous theoretical studies of quasifree electron scattering have used either harmonic-oscillator or square-well potentials to describe the bound-state, single-particle wave functions. In our calculations, in addition to the harmonic-oscillator potential, a Woods-Saxon potential is used which is more realistic, but which requires the use of numerical techniques.

The calculations presented below are the first detailed study of the effects of final-state interactions in quasifree electron scattering. The cross section used takes into account correctly the momentum dependence of the electron-proton interaction and the kinematics of the problem,[13] whereas most other calculations make some simplifying assumptions so that free electron-proton cross sections may be used.

Our results clearly show that the final-state interactions do reduce the size of the cross section except close to diffraction minima. In these areas, they may either fill in or deepen the minimum. Also the cross section is shown to be sensitive to the bound-state potential. The cross sections for the harmonic-oscillator potential are approximately one order of magnitude larger and more peaked than those obtained with the Woods-Saxon potential.

II. DIFFERENTIAL CROSS SECTION

We are interested in the cross section for the reaction $A(e, e'p)B$ shown in Fig. 1. In the initial state, an electron with four-momentum k_i is incident on the target nucleus A. In the final state, the scattered electron with four-momentum k_f is

detected in coincidence with the emitted proton. Our analysis will be based on the first Born approximation, and we restrict ourselves to events in which the nucleons interact as nonrelativistic Pauli particles.

The reduction of the covariant form of the interaction between electrons and nucleons to a two-component form for the nucleons has been done by McVoy and Van Hove.[14] For unpolarized nucleons, and electrons described by plane waves, the two-component Hamiltonian operator in nucleon space which describes the electron-nucleon interaction, correct to second order in inverse nucleon mass, is

$$H = -\frac{e^2}{q_\mu{}^2}\langle U_f | F_1(q_\mu{}^2)\, e^{-iq_\mu x^\mu} - \frac{F_1(q_\mu{}^2)}{2M}(\vec{p}\,\vec{\alpha} e^{-iq_\mu x^\mu} + e^{-iq_\mu x^\mu}\vec{p}\cdot\vec{\alpha}) - \frac{F_1(q_\mu{}^2)+KF_2(q_\mu{}^2)}{2M}$$
$$\times i\vec{\sigma}\cdot(\vec{q}\times\vec{\alpha})\, e^{-iq_\mu x^\mu} + \frac{F_1(q_\mu{}^2)+2KF_2(q_\mu{}^2)}{8M} q_\mu{}^2 e^{-iq_\mu x^\mu} | U_i\rangle \,.$$

In this expression, q_μ is the four-momentum transfer with $q_\mu{}^2 = \omega^2 - |\vec{q}|^2$ where $\vec{q} = \vec{k}_i - \vec{k}_f$ and $\omega = E_i - E_f$. The matrix $\vec{\alpha}$ is the usual Dirac operator, which operates on the free-electron spinors $|U_i\rangle$ and $|U_f\rangle$, $\vec{p}$ and $\vec{\sigma}$ are the momentum and Pauli spin operators in the nucleon space, $F_1(q_\mu{}^2)$ and $F_2(q_\mu{}^2)$ are the nucleon charge and magnetic form factors, and K is the nucleon anomalous magnetic moment in nuclear magnetons.

The interaction Hamiltonian, as given above, is for single-nucleon scattering, and since we are interested in scattering from many-nucleon systems we make the usual assumption that nucleons inside a nucleus do not distort one another so that we can use free-nucleon form factors. For the small values of $q_\mu{}^2$ of interest here, we can use the relation[15]

$$F_1(q_\mu{}^2) = F_2(q_\mu{}^2) = F(q_\mu{}^2).$$

With the above considerations, the Born-approximation matrix element is

$$M_{fi} = \langle \psi_f | \sum_{j=1}^{A} H^{(j)} \Lambda_p^{(j)} | \psi_i \rangle ,$$

where ψ_i and ψ_f are the initial and final time-independent nuclear states, and Λ_p is the proton projection operator.

The coincidence cross section in the lab frame is

$$\frac{d^3\sigma}{dE_f d\Omega_f d\Omega_p} = \frac{2\pi m^2}{E_i E_f} |M_{fi}|^2 \rho_f ,$$

where m is the electron mass. The density of final states, ρ_f, is given by

$$\rho_f = 2(\pi)^{-6} \frac{E_p E_f{}^2 p}{1 - E_p/E_B[(\vec{q}\cdot\vec{p}/p^2) - 1]} ,$$

where

$$E_p = (|\vec{p}|^2 + M^2)^{1/2},$$

and

$$E_B = [\vec{p}_B{}^2 + (A-1)^2 M^2]^{1/2} .$$

In order to evaluate M_{fi}, we need to know the initial and final nuclear wave functions. It is convenient to introduce the center-of-mass and relative coordinates shown in Fig. 2, and defined by

$$\vec{R} = [1/M + M_B)](M_B \vec{R}_B + M\vec{r}_p) \text{ and } \vec{r} = \vec{r}_p - \vec{R}_B .$$

For the final nuclear wave function, we take

$$\psi_f = \Phi_B(\vec{x}_B)\chi(\vec{r})\, e^{i\vec{K}\cdot\vec{R}} | \tfrac{1}{2} m_f \rangle ,$$

where $\Phi(\vec{x}_B)$ is the wave function of the residual nucleus, and $\chi(\vec{r})$ is the wave function for the relative motion of the residual nucleus and the outgoing proton. The plane wave describes the motion of the center-of-mass of the total system, where $\vec{K}$ is the total momentum of the residual nucleus and outgoing proton, and $| \frac{1}{2} m_f \rangle$ is the spin wave function for the proton.

For the initial wave function, we take

$$\psi_i = \sum_\alpha C_\alpha \Phi_\alpha(\vec{x}_B) \Big[U_{nl}(r) \sum_{M_L m_i} C^{L\frac{1}{2}J}_{m_L m_i m_J} Y_L{}^{m_L}(\hat{r}) | \tfrac{1}{2} m_i \rangle \Big]_\alpha ,$$

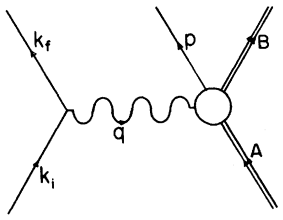

FIG. 1. Diagram for the reaction $A(e, e' p)B$

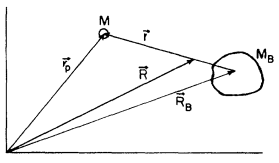

FIG. 2. Laboratory frame for the nuclear system.

where $\Phi_\alpha(\vec{x}_B)$ is the wave function of the nucleons which make up the residual nucleons when still in the initial state, and the expression in brackets describes the relative motion of this nucleon cluster with the proton which will be knocked out. The expression in brackets is a shell-model wave function for the proton moving in some central potential.

By selecting the energy of the final proton, one can determine the initial state from which the proton was ejected. We will assume that this proton moves in a pure central potential so that we can neglect all coupling except the spin-orbit coupling contained in the expression in brackets. By making the additional assumption that the wave functions denoted by Φ_α form an orthonormal set, we can drop the sum on α since only the particular term in which $\Phi_\alpha = \Phi_B$ will contribute to the cross section. The sum on j in M_{fi} is also no longer necessary, because we are considering only a particular proton in the initial state.

For comparison with later results, we will first derive the form of the coincidence cross section obtained when the final-state interactions are neglected. In this case, the square of the matrix element is given by

$$|M_{fi}|^2 = \frac{\pi}{m^2}(e^2/q_\mu{}^2)^2 \Lambda |\, F(n, L, P_B)|^2\, F(q_\mu{}^2)^2,$$

where

$$\Lambda = (4E_i E_f + q_\mu{}^2)\left[1 + \frac{q_\mu{}^2}{8M^2}(1+2K)\right]^2 - \frac{q_\mu{}^2}{8M^2}[(2\vec{p}-\vec{q})^2 + 2(1+K)^2\vec{q}^{\,2}]$$
$$+ \frac{1}{M^2}\{[\vec{k}_i\cdot(2\vec{p}-\vec{q})][\vec{k}_f\cdot(2\vec{p}-\vec{q})] + (1+K)^2(\vec{k}_i\times\vec{q})\cdot(\vec{k}_f\times\vec{q})\} - \left\{\frac{2E_i}{M}[\vec{k}_f\cdot(2\vec{p}-\vec{q})]\right.$$
$$\left. - \frac{2E_f}{M}[\vec{k}_i\cdot(2\vec{p}-\vec{q})]\right\}\left[1 + \frac{q^2}{8M^2}(1+2K)\right],$$

and

$$F(n, L, P_B) = \int j_L(P_B r) U_{nL}(r) r^2 dr\,.$$

To include the effects of final-state interactions between the proton and residual nucleus, we write the final relative-motion wave function as

$$\chi(\vec{r}) = 4\pi \sum_{\lambda\nu} i^\lambda U_\lambda(kr) Y_\lambda^{\nu *}(k) Y_\lambda^\nu(\hat{r}),$$

where $U_\lambda(kr)$ satisfies the radial Schrödinger equation for elastic proton scattering from the residual nucleus. The Born-approximation calculation must now be repeated, using $\chi(\vec{r})$ in the form given above instead of a plane wave. The square of the matrix element now becomes

$$|M_{fi}|^2 = \frac{1}{4m^2}\left(\frac{e^2}{q_\mu{}^2}\right)^2 |F(q_\mu{}^2)|^2\, T,$$

where

$$T = (4\pi)^2 \Lambda \sum_{M_L} \Big|\sum_{\lambda\nu}\sum_{lm} (-1)^\lambda i^l Y_\lambda^\nu(\hat{k})\, Y_l^{m*}(\hat{q}) \left(\frac{2l+1}{2\lambda+1}\right)^{1/2} C_{000}^{Ll\lambda}\, C_{M_L m\nu}^{Ll\lambda}\, I(n, L, \lambda, l, q, k)\Big|^2,$$

and

$$I(n, L, \lambda, l, q, k) = \int U_\lambda^*(kr) j_l((\mu/m) qr) U_{nl}(r) r^2 dr.$$

Since T is a convergent series, the cross section can be calculated numerically as described in the next section.

III. CALCULATIONS

Evaluation of the cross section for the case with final-state interactions must be performed numerically. One can check the main elements of this numerical calculation by using the same programs to evaluate the cross section in the Born approximation. To do this, one simply replaces $U_\lambda^*(kr)$ by $j_\lambda(kr)$ in $I(n, L, \lambda, l, q, k)$. The results of this procedure can then be compared with the much simpler analytic expression which one can obtain in the Born approximation. Given below are the various forms used in our calculations for the single-particle wave functions, the final-state interaction potentials, etc. The $q_\mu{}^2$ dependence of the form factors which was used is given by[16]

$$F(q_\mu{}^2) = \frac{1}{1 + q_\mu{}^2/7.5}\,,$$

where q_μ is expressed in inverse Fermis.

The evaluation of the radial integral, $F(n, L, P_B)$, can be done analytically for a harmonic-oscillator shell-model potential; however, for a Woods-Saxon potential, numerical techniques must be used. The general form of the Woods-Saxon potential which was used is

$$V_B(r) = Vf(r, c, a) + w(\vec{\sigma}\cdot\vec{l})\frac{\lambda^2}{2}\frac{1}{r}\frac{df(r, c, a)}{dr} + V_C ,$$

where V_C is the Coulomb potential of a uniformily charged solid sphere of radius $r_C(A\text{-}1)^{1/3}$ and total charge $(Z\text{-}1)e$ for a nucleus of A nucleons and Z protons. The expression

$$f(r, c, a) = (1 + e^{(r-c)/a})^{-1}$$

is generally referred to as the Fermi density function.

The radial wave function $U(kr)$ used in the final-state wave function is taken to be the final-state wave function of a proton elastically scattered from whatever residual nucleus one has. The interaction is given by a Woods-Saxon optical-model potential of the form

$$V_u(r) = -\left[V_1 f(r, c_1, a_1) + iV_2 f(r, c_2, a_2) + 4ia_3 V_3 \frac{df(r, c_3, a_3)}{dr}\right] + (V_4 + iV_5)(\vec{\sigma}\cdot\vec{l})\frac{\lambda^2}{2}\frac{1}{r}\frac{df(r, c_4, a_4)}{dr} + V_C .$$

The general description given above for $V_B(r)$ also applies to $V_u(r)$.

IV. RESULTS AND CONCLUSIONS

As an application of the theory presented above, the reaction $C^{12}(e, e'p)B^{11}$ was studied. The binding energies of the protons in C^{12} were taken as 36 and 16 MeV for the $1s_{1/2}$ and $1p_{3/2}$ states, respectively. The final electron energy was fixed at 475 MeV, and the incident electron energy was taken to be 635 MeV for the s state and 605 MeV for the p state. The laboratory angle of the scattered electron θ_e was taken to be 51°. The values were chosen to correspond with the experimental work of Amaldi *et al.*,[17] so that our results could be compared to experimental data. No attempts were made to vary these quantities, since these effects have already been studied by Devanathan.[13]

The optical-model parameters were taken from the results of Glassgold and Kellogg[18] who elastically-scattered 95-MeV protons from C^{12}. These parameters were held fixed throughout the calculations, while the parameters in the bound-state potential were varied to obtain best fits with the experimental data.

Figures 3 and 4 are semilog plots of the differential cross section versus the proton scattering angle for quasifree electron scattering from C^{12},

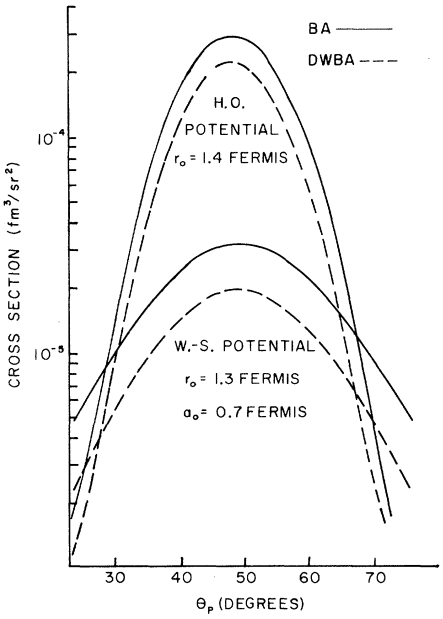

FIG. 3. Cross sections for quasifree electron scattering from C^{12} with protons in the $1s_{1/2}$ state knocked out.

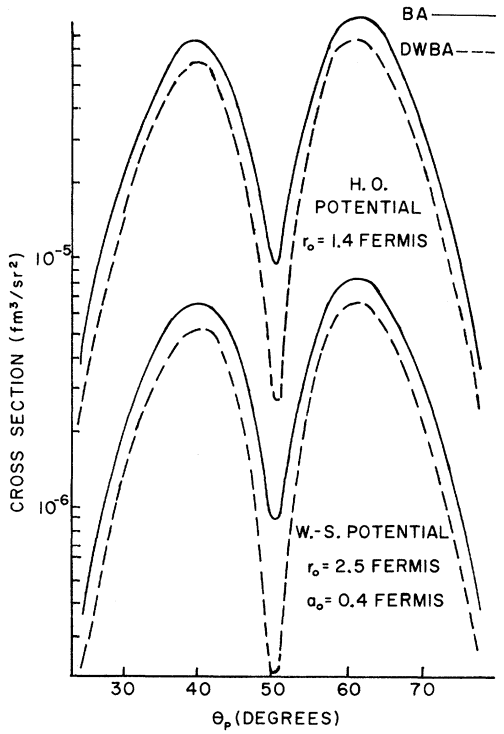

FIG. 4. Cross sections for quasifree electron scattering from C^{12} with protons in the $1p_{3/2}$ state knocked out.

with protons knocked out of the s and p states, respectively. In each case, the top two curves are for the harmonic-oscillator bound-state potentials and the bottom two are for Woods-Saxon potentials. In all graphs, the solid lines are for Born-approximation calculations and the dashed lines include the effects of final-state interactions. The cross sections using the Woods-Saxon bound-state potential are generally smaller than the corresponding cross sections using the harmonic-oscillator potential. Also the harmonic-oscillator case is more peaked, as one would expect, because of the rapid fall-off of the harmonic-oscillator wave functions. The final-state interactions generally reduce the size of the cross section, and around the diffraction minimum this reduction is greatest.

In Figs. 5 through 8, only angular distribution results are shown, so the cross sections are given in arbitrary units. Following Amaldi *et al.*,[17] the cross sections are plotted as a function of the recoil momentum of the residual nucleus, and in all eight figures the experimental points are included for purposes of comparison. The fitting procedure in all cases was simply to normalize the curve to approximately the same maximum as the experimental data.

Figure 5 shows the best fit to the experimental data for the Woods-Saxon bound-state potential with protons in the p state knocked out. The half-radius parameter r_0 necessary to get this fit was quite large, having the value $r_0 = 2.5$ F or $c = 2.5A^{1/3} = 5.73$ F. The cross section is insensitive to variations in the diffuseness a, or the spin-orbit parameter w; however, it is very sensitive to variations in r_0.

Figure 6 shows similar results for the harmonic-oscillator bound-state potential. The oscillator constant necessary to give the best fit corresponds to a nuclear radius parameter of $r_0 = 1.4$ F.

Final-state interactions do not contribute significantly to the angular distributions of the cross sections for protons knocked out of the s state of C^{12}, as can be seen in Figs. 7 and 8. From these two curves we see that the Woods-Saxon bound-state potential fits the experimental data very nicely for the s-state protons, whereas, for the harmonic-oscillator potential, the shape of the curves is not in agreement with the experimental data.

To illustrate further the methods presented in Secs. II and III, a calculation was made for the reaction $Ca^{40}(e, e'p)K^{39}$ for protons knocked out of the $1p_{3/2}$ state. This result is shown in Fig. 9. The optical-model parameters were taken from the results of Barrett, Hill, and Hodgson.[19] The binding energy was taken as 32 MeV.[3] In this case, the final-state interactions still greatly reduce the

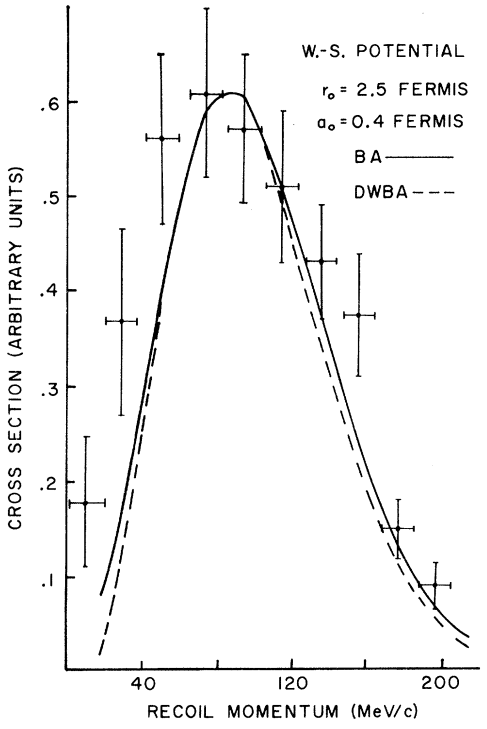

FIG. 5. Angular-distribution results with a Woods-Saxon bound-state potential for p-state protons removed from C^{12}.

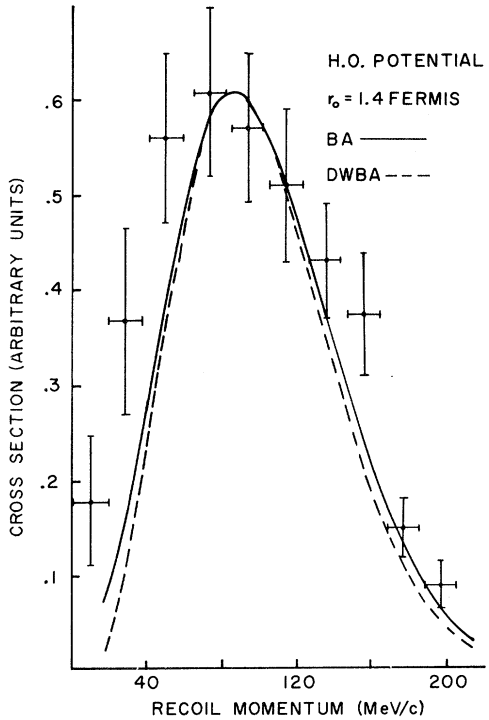

FIG. 6. Angular-distribution results with a harmonic-oscillator bound-state potential for p-state protons removed from C^{12}.

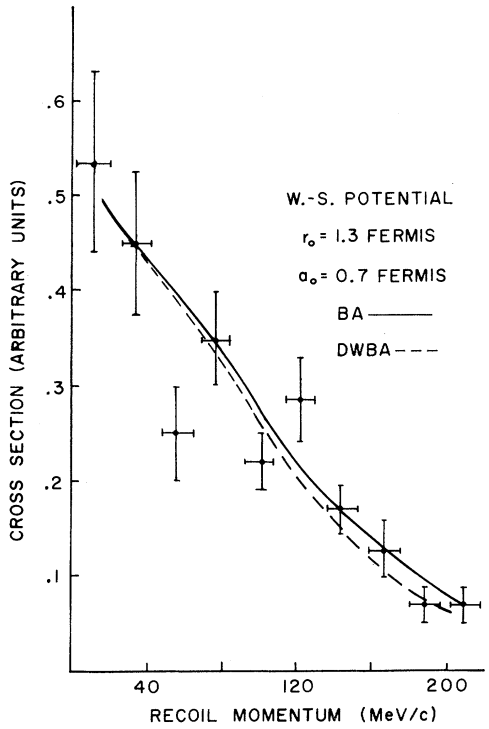

FIG. 7. Angular distribution results with a Woods-Saxon bound-state potential for s-state protons removed from C^{12}.

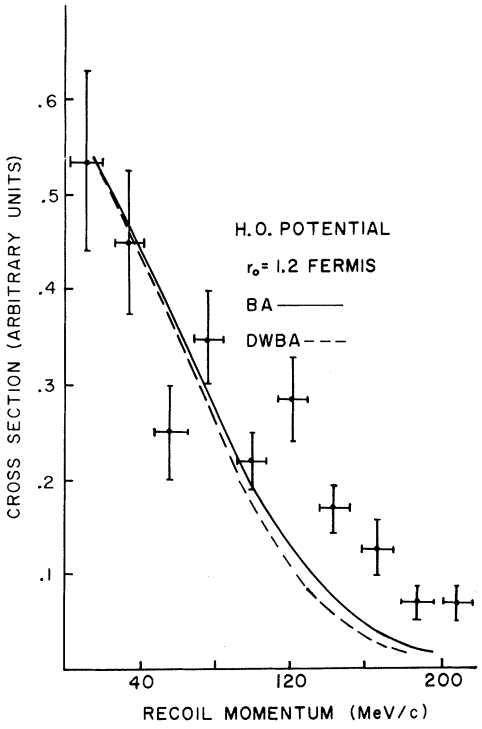

FIG. 8. Angular distribution results with a harmonic-oscillator bound-state potential for s-state protons removed from C^{12}.

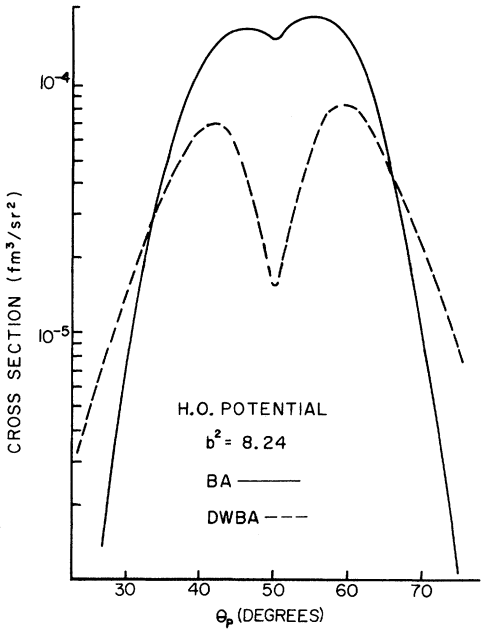

FIG. 9. Cross sections for quasifree electron scattering from Ca^{40} with protons in the $1p_{3/2}$ state knocked out.

minimum; however, here the peaks are shifted away from the minimum.

It has been shown by Degli Atti[20] that elastic electron scattering results from C^{12} are inconsistent with quasifree scattering results. Figure 10 shows a plot of the C^{12} form factor obtained using the Woods-Saxon bound-state wave functions which give the best fit to quasifree scattering results. The fact that the curve falls lower than the experimental points is to be expected, because of the large nuclear-radius parameter used for the p-state wave functions.

Two general conclusions can be drawn from these results. First, the use of a reduction factor to account for the effects of final-state interactions is a good approximation for C^{12}. Second, the popular opinion that final-state interactions should fill in the differential cross section in the region of the diffraction minimum is not necessarily so. The results presented above clearly show the reverse effect.

In order to get a qualitative understanding of this apparent discrepancy, we consider the matrix element of the cross section. Formally, we can write this matrix element as

$$M = M_B + M_C ,$$

where M_B is the matrix element for the Born approximation and M_C is the matrix-element correction which comes from including final-state interactions. In what follows, we will only be interested in the region around the diffraction minimum,

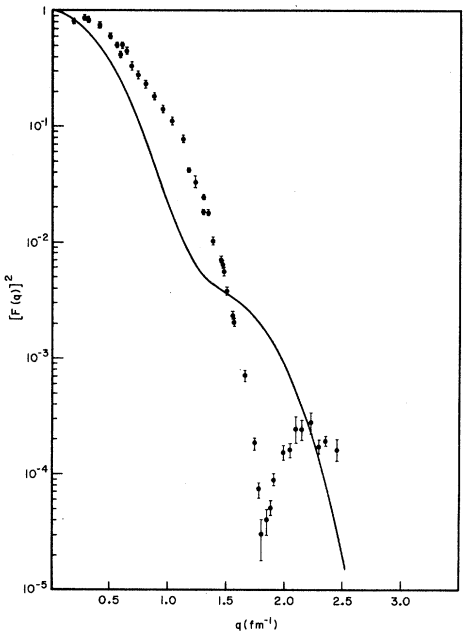

FIG. 10. The elastic form factor of the C^{12} nucleus computed using Woods-Saxon bound-state wave functions which give the best fit for quasifree scattering.

and for purposes of discussion we assume M_C is slowly varying. The minimum in M_B is zero for one particular value of q, and, if we assume M_C is nonzero at this point, it is clear that the diffraction minimum must be filled in for this value of q. As q is varied away from this point in one direction, the magnitude of the matrix element will be increased, and in the other direction it will be decreased. A study of this effect was made by varying the value of E_f from 580 to 660 MeV and plotting the values of ϵ at the diffraction minima against E_f, where

$$\epsilon = \frac{\sigma_{BA} - \sigma_{DWBA}}{\sigma_{DWBA}} .$$

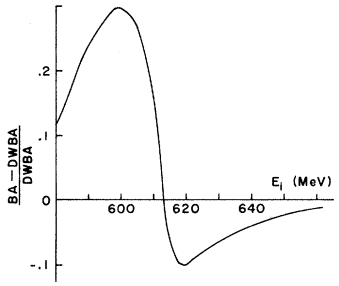

FIG. 11. Variations between the Born-approximation cross sections and the distorted-wave Born-approximation cross sections at the diffraction minimum.

This graph is shown in Fig. 11.

The calculations presented in Sec. II, although computationally long, are generally applicable to any quasifree electron scattering reaction. Until more experimental results become available, one cannot know if a reduction factor will successfully account for the effects of final-state interactions in all these reactions, or if a more general calculation like the one described will be necessary. The question of filling or deepening the diffraction minimum is only of theoretical interest, since experimental results will always fill the minimum because of the angular resolution of the detectors.

*Work supported in part by the U. S. Atomic Energy Commission.

[1]G. Jacob and Th. A. J. Maris, Rev. Mod. Phys. 38, 121 (1966).

[2]U. Amaldi, Jr., Atti Accad. Nazl. Lincei, Rend. Classe Sci. Fis. Mat. Nat. 41, 494 (1966).

[3]U. Amaldi, Jr., G. Campos Venuti, G. Cortellessa, E. De Sanctis, S. Frullani, R. Lombard, and P. Salvadori, Phys. Letters 22, 593 (1966).

[4]U. Amaldi, Jr., G. Campos Venuti, G. Cortellessa, G. Fronterotta, A. Reale, and P. Salvadori, Atti Accad. Nazl. Lincei, Rend. Classe Sci. Fis. Mat. Nat. 39, 470 (1965).

[5]U. Amaldi, Jr., G. Campos Venuti, G. Cortellessa, G. Fronterotta, A. Reale, and P. Salvadori, Atti Accad. Nazl. Lincei, Rend. Classe Sci. Fis. Mat. Nat. 38, 499 (1965).

[6]U. Amaldi, Jr., G. Campos Venuti, G. Cortellessa, C. Fronterotta, A. Reale, P. Salvadori, and P. Hillman, Phys. Rev. Letters 13, 341 (1964).

[7]M. Croissiaux, Phys. Rev. 127, 613 (1962).

[8]A. Johansson, Phys. Rev. 136, B1030 (1964).

[9]P. Bounin, Ann. Phys. (Paris) 10, 475 (1965).

[10]G. Jacob and Th. A. J. Maris, Nucl. Phys. 31, 139 (1962).

[11]A. Wyatt, Phys. Letters 27B, 190 (1968).

[12]T. A. Griffy, R. J. Oakes, and H. M. Schwartz, Nucl. Phys. 86, 313 (1966).

[13]V. Devanathan, Ann. Phys. (N.Y.) 43, 74 (1967).

[14]K. W. McVoy and L. Van Hove, Phys. Rev. 125, 1034 (1962).

[15]R. Hofstadter, Rev. Mod. Phys. 28, 214 (1956).

[16]E. B. Hughes, T. A. Griffy, M. R. Yearian, and R. Hofstadter, Phys. Rev. 139, B458 (1965).

[17]U. Amaldi, Jr., G. Campos Venuti, G. Cortellessa, E. De Sanctis, S. Frullani, R. Lombard, and P. Salvadori, Phys. Letters 25B, 24 (1967).

[18]A. E. Glassgold and P. J. Kellogg, Phys. Rev. 109, 1291 (1958).

[19]R. C. Barrett, A. D. Hill, and P. E. Hodgson, Nucl. Phys. 62, 133 (1965).

[20]C. C. Degli Atti, Nucl. Phys. A106, 215 (1968).